



Supplement of

Study on the influence of topography on wind shear numerical simulations based on WRF–CALMET

Xingyu Wang et al.

Correspondence to: Jinyan Wang (wangjny@lzu.edu.cn)

The copyright of individual parts of the supplement might differ from the article licence.

Supplement

1

2 1. Calmet model introduction

3 CALMET employs a two-step method to compute the wind field(Scire J S et
4 al,2000). In the first step, the initial guessed wind field is adjusted based on the
5 kinematic impacts of terrain, blocking effects, and slope flow. The second step
6 involves incorporating observational data into the wind field derived from step 1
7 using an objective analysis procedure. CALMET, as a three-dimensional microscale
8 meteorological diagnostic model, incorporates the kinematic impacts of terrain on
9 vertical velocity and horizontal wind components, the influence of terrain on wind
10 field dynamics, and the thermodynamic blocking effects of terrain on wind field
11 dynamics. The simulation of near-surface winds in the model is highly sensitive to the
12 localized effects caused by the uneven nature of terrain and the Earth's surface.

13 2. Calculation method of wind shear

14 According to ICAO's recommended standards for vertical shear strength of
15 horizontal wind, wind shear affecting aircraft is classified into four grades based on
16 the vertical thickness of the air layer(NO A): mild (0-2 m/s/30m), moderate (2.1-4
17 m/s/30m), strong (4.1-6 m/s/30m), and severe (above 6 m/s/30m). In this study,
18 wind shear is computed for each layer at intervals of 10 meters (m/s/10m) for
19 consistency in units across different altitude layers. This standardization facilitates a
20 uniform assessment of wind shear intensity.

21 To ensure consistency in data, the wind speed in WRF is interpolated from the
22 PH layers to the height layers of the CALMET model. This interpolation aligns the
23 wind fields simulated by both models on the same set of vertical layers. Subsequently,
24 the following method is employed to calculate VWS:

25 Let s_1 and s_2 represent the total wind speeds in the upper and lower layers,
26 respectively. Also, let θ denote the difference in wind direction between the upper
27 and lower layers. The formula for calculating the vertical wind shear β is given by:

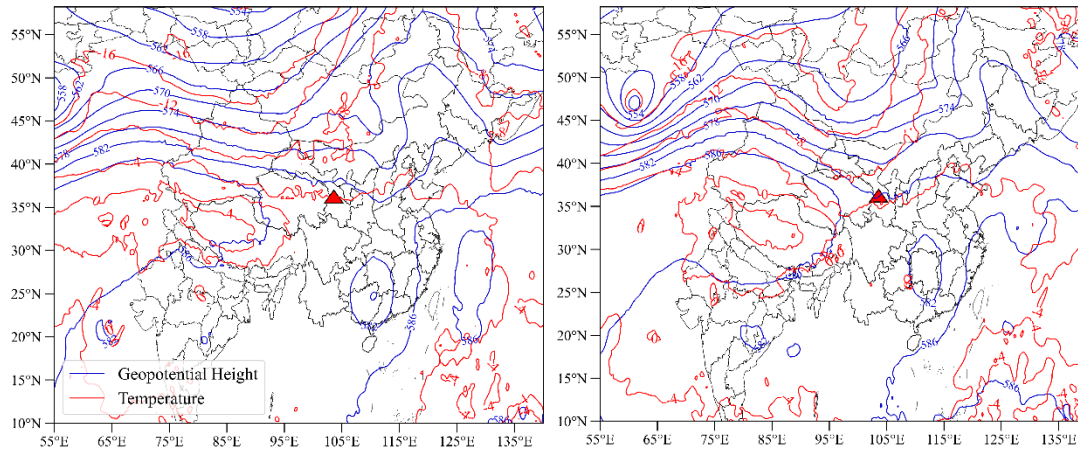
$$28 \quad \beta = \sqrt{s_1^2 + s_2^2 - 2s_1s_2\cos\theta} \quad (4)$$

29 Where:

$$30 \quad s_1^2 = u_1^2 + v_1^2, s_2^2 = u_2^2 + v_2^2, \theta = |\theta_1 - \theta_2|, \theta_1 = \arctan\left(\left|\frac{u_1}{v_1}\right|\right), \theta_2 = \arctan\left(\left|\frac{u_2}{v_2}\right|\right)$$

31

3. Description of weather process

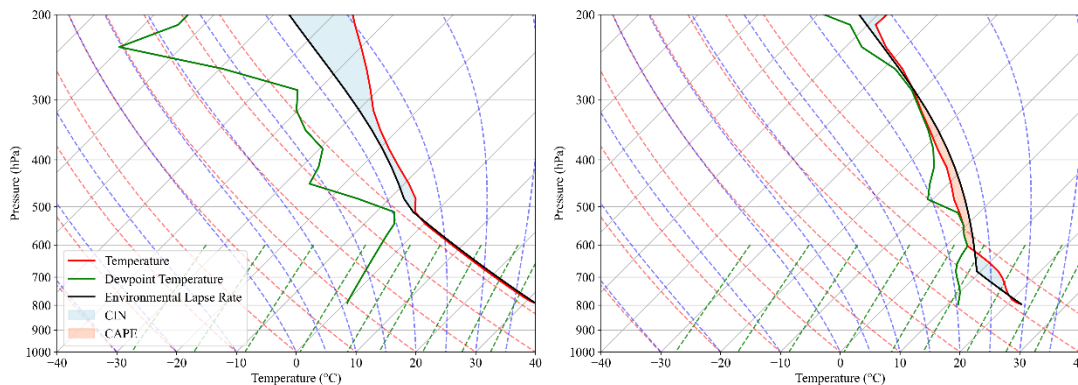


32

33

(a)

(b)



34

35

(c)

(d)

36 *Figure S1. Atmospheric Circulation Patterns at 500hPa and Skew-T Diagrams for*
 37 *Lanzhou Zhongchuan Airport on July 3, 2022, at 08:00 (a)(c) and July 4, 2022, at 08:00*
 38 *(b)(d). (a)(b) High-altitude circulation forms at 500hPa, (c)(d) Skew-T diagrams for*
 39 *Lanzhou Zhongchuan Airport. The triangular marker indicates the location of*
 40 *Lanzhou Zhongchuan Airport.*

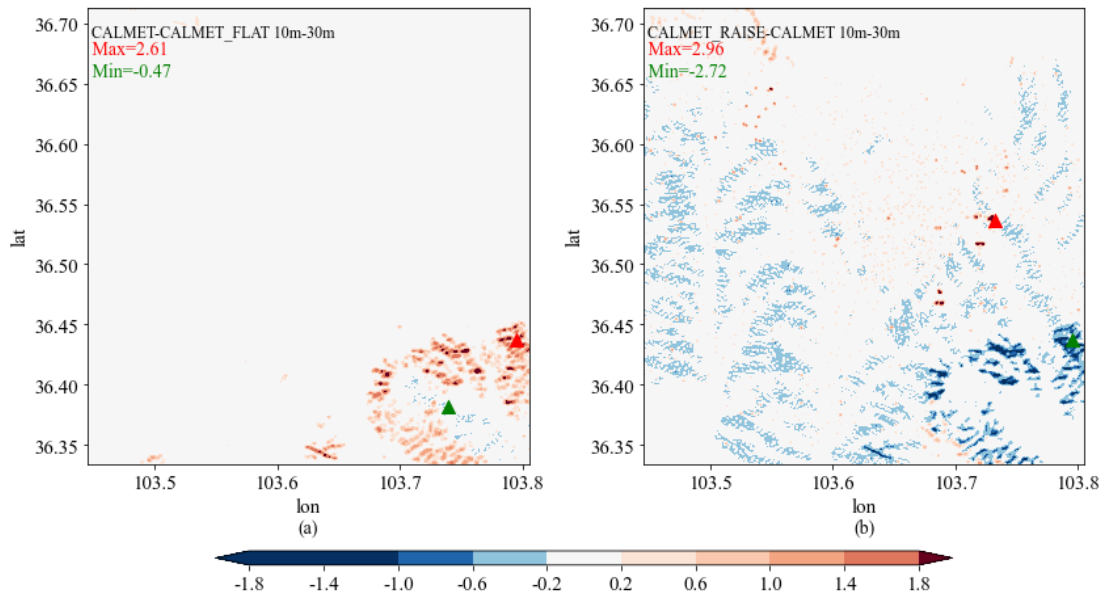
41 From July 3rd to 5th, 2022, a severe convective event occurred near Zhongchuan
 42 Airport. Figure S1(a) and (b) depict the geopotential height and temperature fields at
 43 500hPa on July 3, 2022, at 08:00 (before convective development) and on July 4, 2022,
 44 at 08:00 (during convective development). Before convective initiation, there was a
 45 closed cold low-pressure center near the Caspian Sea. The system of two troughs and
 46 two ridges in the East Asia region shifted eastward. The low-pressure trough at the
 47 location of Zhongchuan Airport deepened, and there was a distinct cold outflow ahead
 48 of the trough. Figures S1(c)-(d) present Skew-T diagrams for the Zhongchuan Airport
 49 area in Lanzhou. On July 3rd at 08:00, only Convective Inhibition (CIN) was observed
 50 without Convective Available Potential Energy (CAPE), indicating the presence of
 51 convective inhibition in the atmosphere, with insufficient available energy to support

52 robust convective development. On July 4th at 08:00, there was CAPE from 620hPa to
53 300hPa, with a numerical value of 285.652 J/kg, and CIN is 111.712 J/kg. A situation
54 where CAPE exceeded CIN is generally favorable for convective development. A
55 higher CAPE value suggested sufficient potential convective energy in the atmosphere,
56 supporting the development of convective clouds. Larger CAPE values were typically
57 associated with more intense convection.

58

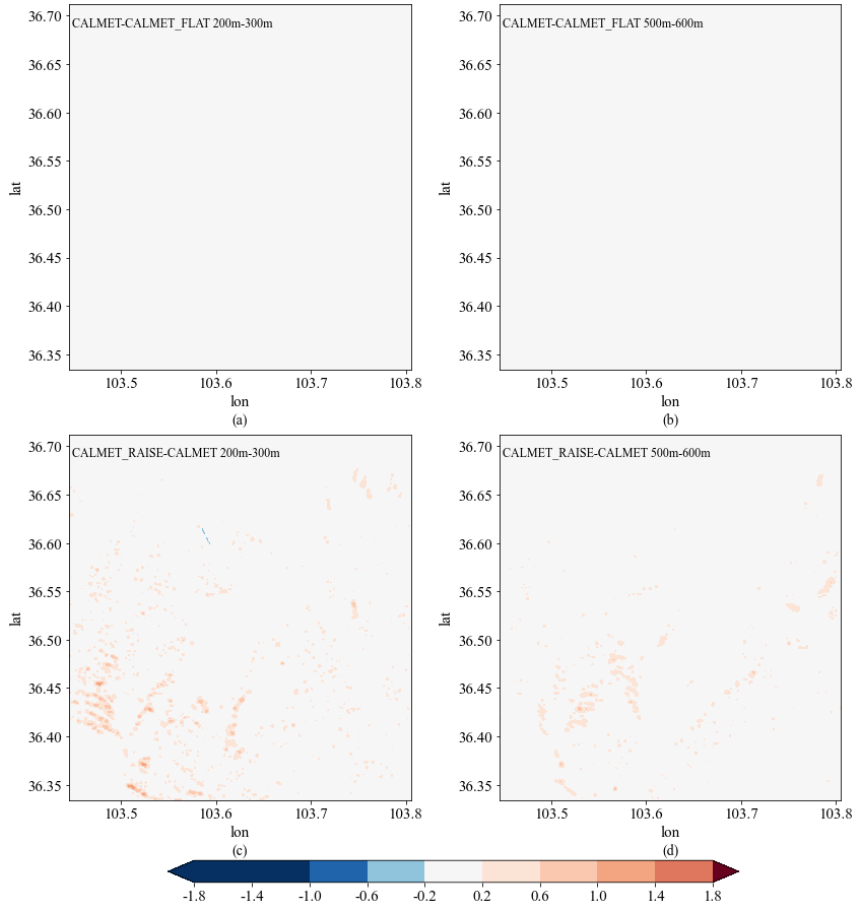
59 4. Supplementary material

60 4.1 Supplementary explanation for Figure 5 in the main text



61

62 *Figure S2: Difference of 30m-10m altitude layer VWS of three experiments at*
63 *19:00 on July 3, 2022 :(a):CALMET-CALMET_FLAT; (b):CALEMT_RAISE-CALMET; The*
64 *red triangle is where the maximum value occurs, and the greentriangle is where the*
65 *minimum value occurs.*



66

67

68

69

70

Figure S3. VWS difference of three experiments at 19:00 on July 3, 2022 : (a),(b):CALMET-CALMET_FLAT; (c),(d):CALEMT_RAISE-CALMET; (a),(c):200m-300m;(b),(d):500m-600m. The red triangle is where the maximum value occurs, and the green triangle is where the minimum value occurs.

71

72

73

74

75

76

77

To visually illustrate the differences among the three experiments and observe the conditions at different height levels, Figure S2 and Figure S3 presents the VWS differences for the three experiments at 19:00 on July 3, 2022. Analyzing the difference between CALMET and CALMET_FLAT, it is evident that in the 10m-30m height range, CALMET's VWS values are significantly higher in the southeast compared to CALMET_FLAT, with minor differences in other locations. In the 200m-300m and 500m-600m height ranges, the disparity between the two is minimal.

78

79

80

81

82

83

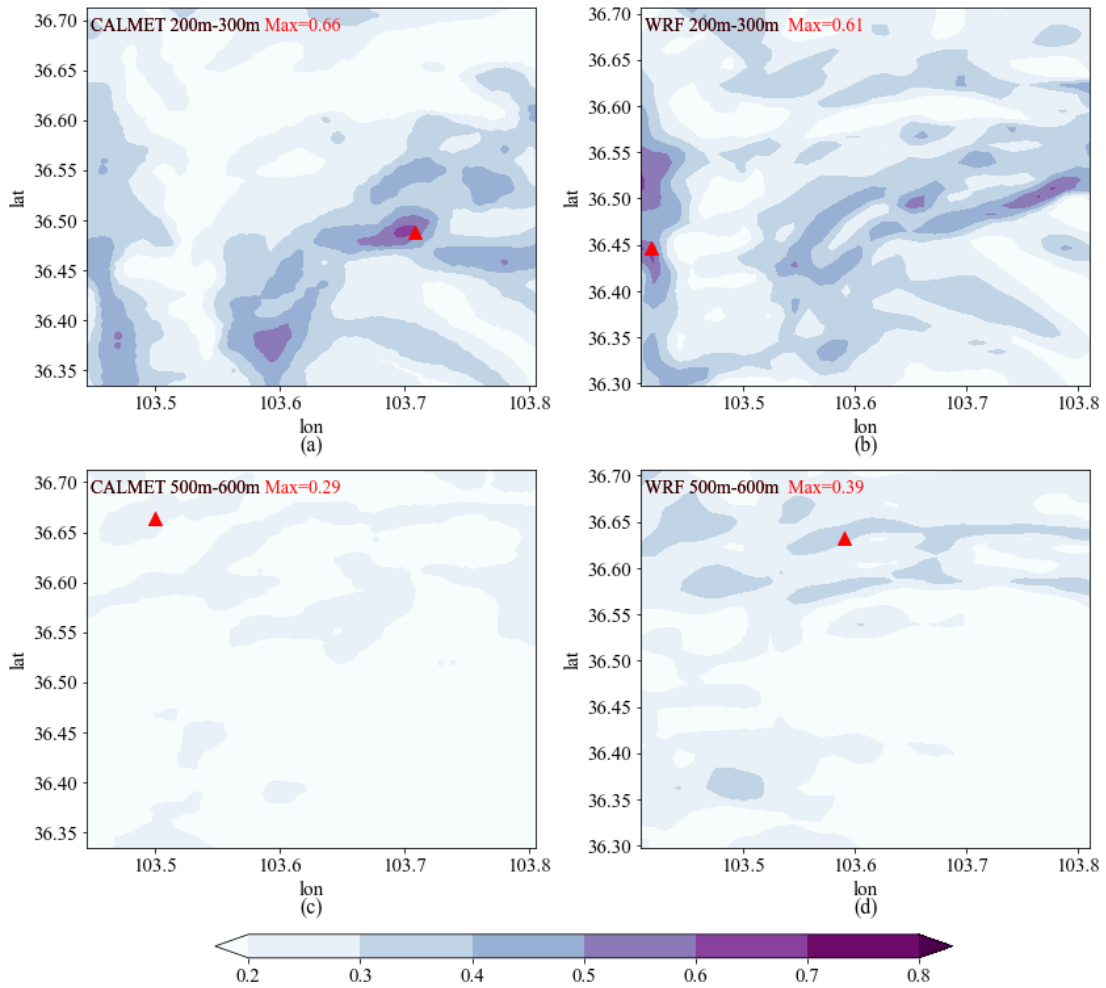
84

85

Examining the difference between CALMET_RAISE and CALMET, in the 10m-30m height range, CALMET generally has slightly higher values than CALMET_RAISE. Notably, in the southeast, CALMET exhibits a pronounced high-value area compared to CALMET_RAISE, with a maximum difference of 2.72 m/s/10m. Conversely, in the central region, CALMET_RAISE shows several high-value point-shaped areas compared to CALMET, with the maximum exceeding CALMET by 2.96 m/s/10m. In the 200m-300m height range, there are small, distinct high-value areas in the southwest, with a maximum of 1.3 m/s/10m and a minimum of 0.22 m/s/10m.

86 Overall, CALMET_RAISE's enhancement is more pronounced than its reduction. In the
87 500m-600m height range, similar to the 200m-300m range, CALMET_RAISE's
88 enhancement is more noticeable than the reduction, but the absolute value of the
89 difference decreases with increasing height.

90 4.2 Supplementary explanation for Figure 5 in the main text



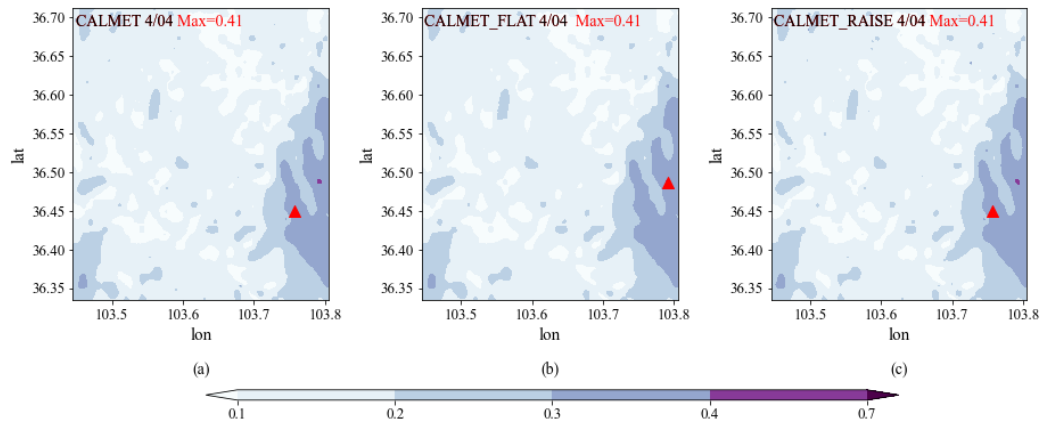
91

92 *Figure S4. VWS at 16:00 on July 3, 2022 (unit: m/s/10m). (a),(c)CALMET;*
93 *(b),(d)WRF; (a),(b): 200-300m VWS; (c),(d) VWS of 500m to 600m indicates the*
94 *location where the maximum value occurs.*

95 In the 200m-300m height layer (Figure S4(a),(b)), the maximum VWS values
96 simulated by both models are similar. CALMET's distribution trend is similar to that
97 of the 10m-30m layer: low values are observed on ridges and in northern
98 mountainous areas, while high values are distributed on the western slopes of the
99 ridges and in valley areas. WRF's maximum VWS values appear on the western slopes
100 of the ridges, with an overall irregular distribution. In the 500m-600m height layer
101 (Figure S4(c),(d)), CALMET's maximum VWS values are generally lower than those of
102 WRF, with instances where CALMET's values are lower than WRF's.

4.3 Simulation of low wind speed periods in the early morning

103
104



105
106
107
108

Figure S5. 10m-30m VWS of CALMET(a), CALMET_FLAT(b) and CALMET_RAISE(c) at 04:00 on July 4, 2022 (unit: m/s/10m). The triangle represents where the maximum value occurs

109 The strong agreement in maximum Vertical Wind Shear (VWS) values among the
110 three experiments during early morning and morning hours is evident. Taking the
111 VWS distribution at 04:00 on July 4 (Figure S5) as an example, the ground-level VWS
112 (10m-30m) shows consistent patterns across all three experiments, with maximum
113 values consistently located in the flat river valley to the east. This indicates minimal
114 terrain impact on VWS simulation by the CALMET model during these time periods.

115 Valley winds typically influence VWS significantly over complex mountainous
116 terrain. However, in flat river valley areas, observed in these experiments, terrain
117 changes are minimal, exerting little influence on VWS. This suggests the model
118 accurately reflects atmospheric motion in flat regions, boosting confidence in VWS
119 distribution.

120

121 **References**

122

123 NO, A.: MANUAL ON LOW-LEVEL WIND SHEAR,

124 Scire, J. S., Robe, F. R., Fernau, M. E., and Yamartino, R. J.: A user's guide for the CALMET
125 Meteorological Model, Earth Tech, USA, 37, 2000.